

1 **Quantum aspects of evolution: a contribution toward evolutionary explorations of**  
2 **genotype networks via quantum walks**

3

4 Diego Santiago-Alarcon<sup>1\*</sup>, Horacio Tapia-McClung<sup>2\*</sup>, Sergio Lerma-Hernández<sup>3</sup>, Salvador  
5 E. Venegas-Andraca<sup>4</sup>

6

7 <sup>1</sup> Red de Biología y Conservación de Vertebrados. Instituto de Ecología, A.C. Carr.  
8 Antigua a Coatepec 351, Col. El Haya. C.P. 91070. Xalapa, Veracruz, México.

9

10 <sup>2</sup> Centro de Investigación en Inteligencia Artificial, Universidad Veracruzana. Sebastián  
11 Camacho 5, Centro, Xalapa-Enríquez, Veracruz, México.

12

13 <sup>3</sup> Facultad de Física, Universidad Veracruzana. Circuito Aguirre Beltrán s/n, Xalapa,  
14 Veracruz 91000, México

15

16 <sup>4</sup> Tecnológico de Monterrey, Escuela de Ingeniería y Ciencias. Ave. Eugenio Garza Sada  
17 2501, Monterrey 64849, NL, Mexico.

18

19 \*Corresponding authors: [diego.santiago@inecol.mx](mailto:diego.santiago@inecol.mx); [htapia@uv.mx](mailto:htapia@uv.mx)

20

21

22

23

24

25 **Abstract**

26

27 Quantum biology seeks to explain biological phenomena via quantum mechanisms, such as  
28 enzyme reaction rates via tunneling and photosynthesis energy efficiency via coherent  
29 superposition of states. However, less effort has been devoted to study the role of quantum  
30 mechanisms in biological evolution. In this paper, we used transcription factor networks  
31 with two and four different phenotypes, and used classical random walks (CRW) and  
32 quantum walks (QW) to compare network search behavior and efficiency at finding novel  
33 phenotypes between CRW and QW. In the network with two phenotypes, at temporal  
34 scales comparable to decoherence time  $T_D$ , QW are as efficient as CRW at finding new  
35 phenotypes. In the case of the network with four phenotypes, the QW had a higher  
36 probability of mutating to a novel phenotype than the CRW, regardless of the number of  
37 mutational steps (i.e., 1, 2 or 3) away from the new phenotype. Before quantum  
38 decoherence, the QW probabilities become higher turning the QW effectively more  
39 efficient than CRW at finding novel phenotypes under different starting conditions. Thus,  
40 our results warrant further exploration of the QW under more realistic network scenarios  
41 (i.e., larger genotype networks) in both closed and open systems (e.g., by considering  
42 Lindblad terms).

43 **Key words:** quantum biology, quantum evolution, genotype networks, evolutionary  
44 biology

45

46

47

48

## 49 **Background**

50

51 Quantum biology is a novel discipline that uses quantum mechanics to better describe and  
52 understand biological phenomena (Mohseni 2014; Brookes 2017; McFadden and Al-Khalili  
53 2018). Over the last 15 years, there have been theoretical developments and experimental  
54 verifications of quantum biological phenomena (McFadden and Al-Kahlili 2014; Brookes  
55 2017) such as quantum tunneling effects for the efficient workings of enzymes at  
56 accelerating biological metabolic processes (e.g., Klinman and Cohen 2013), and quantum  
57 superposition for efficient energy transfer in photosynthesis (Panitchayangkoon et al.  
58 2010). The area of quantum evolution (McFadden and Al-Kahlili 1999), in which it is  
59 suggested that DNA base pairs remain in a superposition by sharing the proton of hydrogen  
60 bonds, still remains speculative and has practically stagnated since its theoretical inception  
61 twenty years ago (Ogryzko 1997; McFadden and Al-Kahlili 1999). However, recent  
62 theoretical developments on quantum genes (e.g., Brovarets' and Hovorun 2015) suggest  
63 that further exploration of the superposition mechanism in evolution is worth undertaking.

64

65 *Theoretical framework: a) quantum measurement device*

66 From biological principles, genes do not vary in a continuous fashion, they are digital  
67 objects (i.e., a sequence of discrete nucleotides); such discontinuity renders mutations as  
68 quantum jumps between different states or possible variations of a gene (Schrödinger 1944;  
69 Godbeer et al. 2015). In other words, genes function as discrete packets, which are akin to  
70 quantum digital objects over which computations are performed (Lloyd 2008). Hence, the  
71 theoretical framework of quantum mechanics offers two characteristics that are

72 fundamental for life and its evolution: digitalization and probabilistic variation among the  
73 discrete states a quantum system can take (e.g., DNA nucleotides; Lloyd 2008).

74

75 Focusing on DNA, the genetic code is ultimately determined by hydrogen bonds of protons  
76 shared between purine and pyrimidine nucleotide bases (McFadden and Al-Khalili 1999).

77 Nucleotides have alternative forms known as tautomers, where the positions of the  
78 hydrogen protons in the nucleotide are swapped, changing nucleotides chemical properties

79 and affinities (Watson and Crick 1953a,b). Such changes make the DNA polymerase  
80 enzyme to sometimes pair wrong nucleotides (e.g., a tautomeric thymine with a guanine),

81 generating mutations that change the genetic information and possibly the encoded protein  
82 (McFadden and Al-Khalili 1999, 2014; Fig. 1). An important consequence of this process,

83 since genes can be thought of as quantum systems, is that nucleotides' hydrogen bridges  
84 can be described as a quantum superposition, where protons can be found at both sides of

85 the DNA chain at the same time (i.e., the physical variable in a superposition is the  
86 hydrogen proton joining DNA nucleotides; quantum genes), hence allowing the system to

87 be described by a wave function (McFadden and Al-Kahlili 1999, Godbeer et al. 2015). A  
88 measurement (e.g., a chemical, UV light from the environment) can collapse the wave

89 function producing either a normal base pair or a mutation (McFadden and Al-Kahlili 1999,  
90 2014). Thus, quantum processes can be of relevance in the generation of mutations (i.e.,

91 adaptive mutations) when influenced by the surrounding environment (i.e., selective  
92 factors; Brovarets' and Hovorun 2015; Godbeer et al. 2015; Fig. 2), playing an important

93 role in the exploration of evolutionary space (e.g., n-dimensional genotype networks, as  
94 introduced shortly in this manuscript).

95

96 *Theoretical framework: b) n-dimensional genotype networks*

97

98 A theory based on n-dimensional genotype space at different levels of biological  
99 organization (e.g., metabolism, gene regulation) has been developed to understand the  
100 evolution of innovations (Wagner 2011, 2014). A genotype network implies the existence  
101 of a vast connected network of genotypes (nodes in a network) that produces the same  
102 phenotype (Schuster et al. 1994). Genotypes in a genotype network can share little  
103 similarity (e.g., lower than 25%) and still produce the same phenotype (Wagner 2011). To  
104 understand the concept of a genotype network we will focus on metabolic reactions  
105 (Wagner 2011; Fig. 3).

106

107 A metabolic genotype is the total amount of chemical reactions that can be performed by  
108 the enzymes synthesized by an organism's genotype (Wagner 2011). If we use digital (i.e.,  
109 binary) categorization, then we can classify a metabolic genotype as a string of binary flags,  
110 indicating if the genotype has the information to synthesize a product that performs a  
111 metabolic reaction (represented by 1) or not (represented by 0; see Fig. 3). From current  
112 information we know there are about  $10^4$  metabolic reactions (no organism can perform all  
113 of them; Samal et al. 2010), in which case we would have in binary space with  $2^{10,000}$   
114 different possible metabolic genotypes, which is a large universe of possibilities available  
115 for evolution to explore (Samal et al. 2010, 2011; Wagner 2014). Hence, the genetic space  
116 of metabolic genotypes is composed of all possible binary strings of length  $10^4$ , in this case  
117 a total of  $2^{10,000}$ . A way to measure differences between two metabolic genotypes in this  
118 vast space is to use the fraction of reactions that are not catalyzed by one genotype in  
119 reference to the other; the letter  $D$  represents such a measure (Rodrigues and Wagner

120 2009). The maximal value  $D = 1$  would be achieved when the two metabolic genotypes do  
121 not have any reaction in common and  $D = 0$  when they have identical metabolic genotypes  
122 (i.e., they would encode the same products or enzymes). Two metabolic genotypes would  
123 be neighbors if they differ only by a single reaction (a 1 in our binary coding of metabolic  
124 genotypes). Hence, the neighborhood of a metabolic genotype is composed by all those  
125 genotypes that differ by exactly one reaction from it; there would be as many neighbors as  
126 there are metabolic reactions (Fig. 4). Considering the different possible metabolisms one  
127 step away from a focal one, each neighborhood would be a large collection of metabolic  
128 genotypes organized in a hyper-dimensional cube. With this we build an n-dimensional  
129 network, where each genotype is a node in the network and the edges represent mutational  
130 steps, nodes connected by an edge differ exactly by one mutation (Rodrigues and Wagner  
131 2009; Wagner 2014; Fig. 4).

132

133 A metabolic phenotype is represented by all the environmental energy sources (e.g.,  
134 glucose, methane) that can be used by a metabolic genotype to synthesize all biomolecules  
135 (e.g., amino acids, nucleotides) required for survival (Fig. 3). The metabolic phenotype can  
136 also be categorized as a binary string, a 1 represents a genotype network that can synthesize  
137 all required biomolecules relying solely on that specific source and a 0 otherwise; a  
138 phenotype with multiple ones means a metabolism that can produce all needed elements  
139 from many different sources (Wagner 2011). To calculate the number of possible  
140 phenotypes, we do the same as for metabolic genotypes; we raise two to the power of all  
141 the known different energy sources available. The set of those metabolic genotypes that  
142 have the same phenotype is what constitutes a genotype network. It has been shown  
143 computationally that similar (i.e., neighbors), as well as very dissimilar genotypes (as

144 different as 80% of their metabolic reactions), can still preserve the same phenotype,  
145 demonstrating that genotype networks are plastic and robust (e.g., Wagner 2008; Rodrigues  
146 and Wagner 2011). This is a good feature for evolving populations because browsing the  
147 vast genotypic space becomes feasible and moderately free of risk (Rodrigues and Wagner  
148 2009, Samal et al. 2010). However, how can new features evolve when a vast exploration  
149 leads us to the same viable result or phenotype? When comparing the neighborhoods of  
150 thousands of pairs of metabolic genotypes that are able to use the same energy source (i.e.,  
151 they belong to the same phenotype network), but that are otherwise very different, it turns  
152 out that their neighborhoods are very different and diverse (i.e., novel phenotypes in one  
153 neighborhood might not be present in other neighborhoods of the same genotype network,  
154 Wagner 2014; Fig. 4). As the number of changed metabolic reactions increases, so does the  
155 number of unique phenotypes in a neighborhood, opening a bounty of novel phenotypes to  
156 an evolving population (Rodrigues and Wagner 2009). Furthermore, when comparing two  
157 genotype networks (i.e., networks that produce different phenotypes), the distance in  
158 genotype space that needs to be traversed to find a novel phenotype is rather small (i.e., the  
159 number of edges or mutational steps in the network separating nodes or genotypes with  
160 different phenotypes), raising the odds of finding novel traits (Wagner 2014, Rodrigues and  
161 Wagner 2011; Fig. 4). More impressive yet is the fact that networks other than metabolism,  
162 such as transcriptional regulatory circuits (Ciliberti et al. 2007, Espinosa-Soto et al. 2011)  
163 and the development of novel molecules (Li et al. 1996, Cui et al. 2002, Bastolla et al.  
164 2003, Sumedha et al. 2007) have the same basic structure (Wagner 2011).

165

166 There is no true randomness as originally conceived in Darwinian evolutionary theory (e.g.,  
167 Cairns et al. 1988; Hall 1995, 1997; Wagner 2012a). A series of experiments have shown

168 that mutations are not completely random and that they can actually happen as a response  
169 to an environmental factor (e.g., Cairns et al. 1988, Rosenberg et al. 1994; Hall 1997, 1998;  
170 Hendrickson et al. 2002; Stumpf et al. 2007; Braun and David 2011; Livnat 2013). Thus,  
171 we are ultimately interested in the potential effect that specific environmental conditions  
172 (i.e., probing agents that collapse the quantum superposition) have on the proposed genetic  
173 quantum system and the evolutionary pathway followed under such conditions (e.g., Fig.  
174 5). Yet, we must first understand how quantum processes behave under non-selective (i.e.,  
175 neutral and in closed systems) scenarios, so we can determine their relevance for evolution.  
176 Thus, in this paper we explore how fast a quantum walk (QW) could explore an n-  
177 dimensional genotype network, *sensu* Wagner 2011 (i.e., a state space) and compare its  
178 performance with that of a classical random walk (CRW) (e.g., Farhi and Gutmann 1998).  
179 Then, we explore under what scenarios of the state space (i.e., mutational steps between  
180 different phenotypes) may the quantum process be more efficient than the classical one at  
181 finding novel states (i.e., phenotypes) in n-dimensional genotype networks (Wagner 2014;  
182 Aguilar-Rodríguez et al., 2017). That is, we provide proof of concept that genotype  
183 networks are the evolutionary fabric on which the earlier proposed quantum wave function  
184 (Ogryzko 1997; McFadden and Al-Khalili 1999) can operate, and then how the quantum  
185 wave function actually operates on such evolutionary fabric.

186

## 187 **Methods**

188

189 QW are more efficient at exploring one dimension (e.g., linear) and two dimension (e.g.,  
190 grid networks) regular networks (i.e., squared) compared to CRW. CRW remains around  
191 the neighborhood where it started expanding diffusively, whereas the superposition of QW



192 produces a probability cloud expanding ballistically throughout the whole network (Kempe  
193 2003; Venegas-Andraca 2012).

194

195 The superposition property of QW would theoretically allow a more efficient exploration  
196 process throughout the network, given the previously proposed conditions by McFadden  
197 and Al-Khalili (1999):

198 1) The cell is a quantum measurement device that constantly monitors the state of  
199 its own DNA molecule. The environment will induce the collapse of the quantum wave  
200 function, rendering the current state of the DNA (i.e., the DNA sequence we actually  
201 observe when we obtain the base pairs of a genome or a gene), indirectly via the influence  
202 of the environment on the cell (e.g., chemical conditions of the cell's membrane and  
203 cytoplasm).

204 2) Following quantum mechanical jargon, the DNA molecule persists in a  
205 superposition of their hydrogen protons binding nucleotides (i.e., the different mutational  
206 options representing the wave function; see Godbeer et al. 2015). For instance, a wave  
207 function evolving to incorporate the correct and incorrect bases in a DNA position, as a  
208 superposition of states (i.e., mutated and unmutated states [e.g., the Cytosine and Thymine  
209 nucleotides in a DNA base pair]) in a daughter DNA strand; that is, the new DNA state  
210 achieved after replication of the genetic material ( $|\Psi_G\rangle$ ) (McFadden and Al-Khalili 1999):

$$|\Psi_G\rangle = \alpha|\Phi_{not\ tunnelled}\rangle + \beta|\Phi_{tunnelled}\rangle$$

211 3) The operational difference between the DNA and the cell is given by nucleotides  
212 (previous equation above) and amino acids, respectively (see McFadden and Al-Khalili  
213 1999):

$$|\Psi_{cell}\rangle = \alpha|\Phi_{not\ tunnelled}\rangle |Cytosine\rangle |Arginine\rangle + \beta|\Phi_{tunnelled}\rangle |Thymine\rangle \\ > |Histidine\rangle$$

214 4) An evolving or new DNA wave function (i.e., the current DNA superposition  
215 after the collapse of the wave function due to environmental influences) must remain  
216 coherent or stable for long enough time to interact with the cell's immediate environment,  
217 so the cell can act as a quantum device (Fig. 2).

218

219 *Genotype network construction*

220

221 We used a subset of the DNA transcription factor genotype networks from the sample file  
222 of Genonets server (<http://ieu-genonets.uzh.ch>; Khalid et al. 2016), which represent  
223 empirical data for the binding affinities of the Ascl2, Foxa2, Bbx, and Mafb transcription  
224 factors (TF) in mice (Badis et al. 2009, Payne and Wagner 2014; Fig. 6). To filter  
225 genotypes with low binding affinities we used the default value of the parameter tau ( $\tau =$   
226 0.35), and we only allowed for single point mutations (i.e., mutations where a letter in the  
227 sequence is changed, no indels were allowed; see <http://ieu-genonets.uzh.ch/learn> for  
228 definitions and tutorials; Khalid et al., 2016). Briefly, each node in the network represents a  
229 genotype with a specific TF phenotype (i.e., Ascl2, Foxa2, Bbx, Mafb), and the edges  
230 joining nodes represent mutational steps (i.e., two nodes joined by an edge are genotypes  
231 differing exactly by one position; in other words, only one mutation separates such nodes;  
232 see Figs. 3 and 4). We extracted the information of the genotype networks generated by  
233 Genonets, and performed all subsequent simulation analyses (described below) using the  
234 Mathematica software (Wolfram Research, Inc., 2020).

235

236 *Genotype network exploration: closed systems (unitary evolution)*

237

238 The n-dimensional genotype networks developed by Wagner and his collaborators use as an  
239 exploration mechanism CRW (Wagner 2011). Here, we used QW in order to explore the  
240 importance of quantum superposition (Farhi and Gutmann 1998; Mülken and Blumen  
241 2011) as an evolutionary exploration device. Exploration of constructed networks was  
242 performed using both a continuous CRW (e.g., Rodrigues and Wagner 2009) and a  
243 continuous QW (Falloon et al., 2017). We used the QSWalk package developed under  
244 Mathematica to perform simulations on genotype networks (Falloon et al., 2017). The  
245 QSWalk package implements both CRW and continuous QW in arbitrary networks based  
246 on the so-called Quantum Stochastic Walk that generalizes quantum and classical random  
247 walks (Falloon et al., 2017).

248

249 For simplicity, we considered undirected and unweighted networks, which were described  
250 by an adjacency matrix  $\mathbf{A}_{ij}$  whose matrix elements are 1 if the nodes  $i, j$  are connected and 0  
251 otherwise. For an undirected network, the adjacency matrix is symmetric  $\mathbf{A}_{ij} = \mathbf{A}_{ji}$ , which  
252 implies that transitions from any pair of neighboring nodes are equally probable  
253 independently of the direction. For each node  $i$ , we define the out-degree  $\text{outDeg}(i) = \sum_{j \neq i} \mathbf{A}_{ij}$ ,  
254 which counts the number of nodes connected to it. The CRW is described by the vector  
255  $\mathbf{p}(t)$  whose components  $p_j(t)$  give the probability of occupancy of node  $j$ . The temporal  
256 evolution of the probability vector is determined by the equation

$$\frac{d\mathbf{p}}{dt} = \mathbf{H}\mathbf{p}$$

257 where  $\mathbf{H}$  is the matrix

$$\mathbf{H}_{ij} = \begin{cases} \gamma \mathbf{A}_{ij}, & i \neq j \\ -\gamma \text{outDeg}(i), & i = j. \end{cases}$$

258  $\gamma$  determines the transition rate between neighbor nodes. We considered CRW beginning in

259 node  $i$ , implying that the components of the initial vector are  $p_k(t=0) = \delta_{\{ki\}}$ .

260

261 For the QW we considered a basis whose elements are associated to each node of the

262 network  $|i\rangle$ . A general pure state can be written as  $|\psi(t)\rangle = \sum_{\{i\}} c_i |i\rangle$ , where  $|c_i|^2$  is the

263 probability of occupancy of node  $i$ . The dynamics of an initial configuration (similar to the

264 CRW, we considered initial states with components given by  $c_k = \delta_{\{ki\}}$ ) is given by the

265 Schrödinger equation

$$\frac{d|\psi(t)\rangle}{dt} = \mathbf{H}|\psi(t)\rangle,$$

266 where  $\mathbf{H}$  is a linear operator whose matrix elements are given by the same matrix

267 introduced above

$$\langle i|\mathbf{H}|j\rangle = \mathbf{H}_{ij}$$

268 We used DNA transcription factor genotype networks with two (410 nodes) and four (927

269 nodes) different phenotypes, a representation of which is shown in Figure 6. Following, we

270 determined the mutation rate,  $\gamma_c$  and  $\gamma_Q$ , for the CRW and the QW respectively.

271

272 *Mutation rate,  $\gamma$*

273

274 The mutation rate between any pair of neighboring nodes is mapped in the QSWalk

275 package by a parameter,  $\gamma$ . For a CRW, the probability of mutation of a given node to a

276 new node for very short times is  $P_m = N_n \times \gamma_c \times t$ , where  $N_n$  is the number of neighboring

277 nodes; in other words, the probability of remaining in the initial node decays exponentially.  
278 The average number of neighbor nodes in the networks used in our simulations is  $N_n \sim 6.4$   
279  $\pm 3.3$ ; therefore the mutation rate per node is  $mr = 6.4 \pm 3.3 \gamma_c$ . Experimental estimation of  
280 this mutation rate (i.e., the rate of mutation of a single gene; Balin and Cascalho 2010)  
281 yields to  $mr = (4-9) \times 10^{-5}$  mutations/base pair/cell generation. Assuming that a bacterial  
282 cell generation lasts around 1000 sec (i.e., ~20 minutes), the mutation rate is  $mr = (4-9) \times$   
283  $10^{-8}$  mutations/base pair/sec, which when equated to  $6.4 \pm 3.3 \gamma_c$  allows obtaining an  
284 estimation of the order of parameter  $\gamma_c$  for the CRW of  $\gamma_c = 10^{-9} \sim 10^{-7}$  (1/sec).

285  
286 In contrast, for a quantum system described by a Hamiltonian, it can be shown that for very  
287 short times, the probability of transition of a given node to a new node grows quadratically  
288 with time (Mandelstam and Tamm 1945),  $P_m = N_n \times (\gamma_Q \times t)^2$ . In order for the QW to be  
289 consistent with the experimental mutation rate mentioned above, we estimate  $\gamma_Q$ , the  
290 mutation probability of a given node to a new node, by equating the quantum probability of  
291 node mutation with the classical probability at the decoherence time  $T_D$  (i.e., we considered  
292  $\gamma_c \times T_D = (\gamma_Q \times T_D)^2$ , which gives  $\gamma_Q^2 = \gamma_c / T_D$ . Thus, to determine  $\gamma_Q$ , an estimation of  $T_D$  is  
293 necessary. According to McFadden and Al-Khalili (1999), a rough estimation of the  
294 decoherence time is  $T_D = 10^0 \sim 10^2$  sec, which allows an estimation of quantum parameter  $\gamma_Q$   
295  $= 10^{-6} \sim 10^{-3}$ . We selected representative values for  $\gamma_c$  and  $\gamma_Q$  to perform our simulations,  $\gamma_c$   
296  $= 10^{-7}$  (1/sec) and  $\gamma_Q = 10^{-4}$  (1/sec).

297  
298 We follow McFadden and Al-Khalili (1999) at using the Zurek model to estimate  
299 the decoherence time of genotypes (nodes in the network) superposition ( $T_D$ )

300

$$T_D \cong t_R \left( \frac{\lambda_T}{\Delta_x} \right)^2, \quad \lambda_T = \frac{\hbar}{\sqrt{2mk_B T}}$$

301 where  $m$  is the mass of a proton in a superposition of two Gaussian wave packets separated  
302 by a distance  $\Delta_x$ , and  $\lambda_T$  is the thermal de Broglie wavelength dependent (Djordjevic  
303 2016).

304

305 For the small network consisting of 410 nodes and two phenotypes, we performed  
306 independent simulation runs with initial conditions that start from every single node of the  
307 Bbx phenotype to the Foxa2 phenotype and compared the probability to find the Foxa2  
308 phenotype as a function of time for CRW and QW, distinguishing the number of mutational  
309 steps (1, 2 or 3) needed to reach the new phenotype.

310

311 For the larger network (927 nodes and 4 phenotypes), we conducted simulations starting at  
312 nodes that were shared between different pair-wise combinations of the four different  
313 phenotypic networks. The aim was to compare the efficiency at which CRW and QW find  
314 novel phenotypes as a function of time (for the quantum process within the decoherence  
315 time  $T_D$  as calculated above) and of the initial position of a node within a genotype network  
316 in terms of the number of mutational steps (i.e., 1, 2 or 3 edges) needed to reach the new  
317 phenotype.

318

## 319 **Results**

320

321 *Two phenotype networks (Bbx and Foxa2; 410 nodes)*

322 For this two-phenotype network, the linear dependence on time of the mutation probability  
323 of the CRW at short times, induces a linear dependence on time of the probability of  
324 mutation to phenotype *Foxa2* from nodes located one mutational step away (Fig. 7). For  
325 nodes located two or three steps away, the growth of the mutation probability to the new  
326 phenotype is slower. The same hierarchy in the probabilities is observed in the QW, the  
327 closer the node is located to the new phenotype the larger the mutation probability to this  
328 phenotype is. Since the probability of an initial node to mutate to its neighboring nodes  
329 grows quadratically in the QW model, the probability of mutation to a new phenotype is  
330 smaller in the QW model for very short times. But at the temporal scale of quantum  
331 decoherence, the CRW and QW probabilities become comparable. Furthermore, for larger  
332 times, QW probabilities become much larger than the classical ones, irrespective of the  
333 distance of the initial node to the new phenotype. These results show that at a temporal  
334 scale comparable or slightly larger than the decoherence time, the QW becomes more  
335 efficient than the CRW at finding the new phenotype.

336

337 *Four phenotype networks (Ascl2, Foxa2, Mafk, and Bbx; 927 nodes)*

338 Similar to the two-phenotype network simulation, for the CRW there is a linear dependency  
339 on the probability of mutating to a novel phenotype as a function of time (Fig. 8). For the  
340 QW at the temporal scale of quantum decoherence, the quadratic dependence of the  
341 probability of mutating makes the quantum process to have a higher probability of mutating  
342 to a novel phenotype under most conditions compared to the CRW. Such behavior was  
343 observed regardless of the number of mutational steps (i.e., 1, 2 or 3) away from the novel  
344 phenotype (Fig. 8), turning the QW effectively more efficient at finding novel phenotypes  
345 under different starting conditions. Furthermore, the QW became more efficient at finding

346 novel phenotypes when the network increased in complexity in terms of the number of  
347 phenotypes and network size (compare QW results from Figs. 7 and 8).

348

## 349 **Discussion**

350

351 The field of quantum biology has steadily grown over the last 15 years, in particular due to  
352 research focused on photosynthesis and enzymatic processes (Brooks 2017). However,  
353 advances on how quantum mechanisms are relevant to biological evolution have stagnated  
354 during the last two decades, most likely due to a lack of an evolutionary framework where  
355 such quantum processes can be studied (but see Martin-Delgado 2012; Asano et al. 2015).  
356 Here, we have suggested that n-dimensional genotype networks (*sensu* Wagner 2011)  
357 represent an ideal ground where the relevance of quantum superposition for evolution can  
358 be explored. We have shown that under neutral scenarios (i.e., non-selective environments  
359 or closed systems) QW become more efficient at the temporal scale of decoherence time  
360 and under more complex scenarios (four-phenotype vs. two-phenotype networks) than  
361 CRW. The QW model has exhibited a more diverse behavior in terms of mutation  
362 probabilities to a novel phenotype, which is readily observed under a varied array of  
363 conditions (i.e., when starting the simulations at 1, 2 or 3 mutational steps away from novel  
364 phenotypes). Interestingly, the efficiency of QW at finding novel phenotypes increased  
365 when the network structure increased in terms of number of phenotypes and size. This  
366 suggests that as network complexity (i.e., number of phenotypes) and size (number of  
367 genotypes or nodes) increases, we can expect the QW mechanism to be a more efficient  
368 exploration device for evolution given its superposition property. Thus, in order to move



369 forward, the next step is to simulate QWs in open systems coupled to the environment, for  
370 example using dissipative Lindblad terms (e.g., Godbeer et al. 2015).

371

372 If QW prove indeed to be more efficient than CRW in an open network system, then  
373 the still controversial theoretical and experimental evidence in favor of adaptive mutations  
374 (e.g., Hall 1995, Palmer 2012, Braun and David 2011, Livnat 2013) would find an  
375 empirical framework supporting them. Of course, our proposal (i.e., quantum evolution on  
376 n-dimensional networks) does not preclude the existence and commonality of Darwinian  
377 random mutations; it only provides a complementary framework to understand currently  
378 suggested adaptive mutations. An example of a theory expanding current evolutionary  
379 understanding of mutations is that of the writing phenotype (Livnat 2013), which suggests  
380 that mutations are non-random in the sense that there is genomic data showing specific  
381 regions with higher rates of mutations due to specific genome structures. Mechanisms  
382 generating such non-random mutations include non-allelic homologous recombination,  
383 non-homologous DNA end-joining, replication-based mechanisms, and transposition (see  
384 Livnat 2013 for details). In the cases of both n-dimensional genotype networks (Wagner  
385 2009) and writing phenotypes (Livnat 2013) there are evolutionary constraints. In other  
386 words, non-random mutations (*sensu* Livnat 2013) are embedded in a genomic context that  
387 is modified as populations change from generation to generation. Hence, context dependent  
388 evolutionary constraints are dynamic because evolution shuffles the genomic context  
389 through time. However, such dynamic process does not necessarily mean that the procedure  
390 is blind to evolutionary direction within those constraints, which is where the quantum  
391 proposed mechanism of exploration on n-dimensional networks needs further study to  
392 determine its relevance. For example, by using dynamic adaptive networks.

393

394 *Philosophical extensions of QW to epigenetics and niche construction*

395

396 Epigenetics investigates the regulatory mechanisms that during development lead to  
397 persistent and inducible heritable changes that do not affect the genetic composition of the  
398 DNA. Some of these changes can actually regulate the function of DNA without changing  
399 its base composition, via for example methyl groups (Jablonka and Lamb 2010). Epigenetic  
400 inheritance refers to those phenotypic variations that do not depend on DNA sequence  
401 variations, and that can be transmitted across generations of individuals (soma-to-soma)  
402 and cell lines (i.e., cellular epigenetic inheritance); such processes can lead to soft  
403 inheritance (Jablonka 2011). There are four basic types of epigenetic inheritance: 1) self-  
404 sustaining regulatory loops, where following the induction of gene activity, the gene's own  
405 product acts as a positive feedback regulator maintaining gene's activity across cell  
406 generations. 2) Structural templating, where preexisting 3D structures serve as models to  
407 build similar structures in the next generation of cells. 3) Chromatin markings, where small  
408 chemical groups (e.g., methyl CH<sub>3</sub>) bind to DNA, altering/controlling gene activity, they  
409 can segregate during DNA replication and be reconstructed in daughter DNA molecules. 4)  
410 RNA-mediated inheritance, where silent transcription states are maintained by interactions  
411 between small RNA molecules and their complementary mRNA and DNA. These states  
412 can be transmitted to cells and organisms via an RNA replication system, also by having  
413 small RNAs modifying heritable chromatin marks, and by inducing heritable gene deletions  
414 (Rassoulzadegan 2011; see Carey 2012 for a gently general introduction to epigenetics).

415

416           What is most relevant for the proposed framework is the fact that environmental  
417 factors (e.g., heat shock, starvation, chemicals, stress in general) can directly (germ line) or  
418 indirectly (somatic alterations) induce developmental modifications via heritable epigenetic  
419 variations, which underlie developmental plasticity and canalization (Nijhout 2003,  
420 Jablonka and Raz 2009, Jablonka 2011). If we implement the n-dimensional network  
421 concept of Wagner (2011) to an epi-genome, we can obtain an epigenetic network on which  
422 the environment can easily induce state changes in the expression and functioning of genes  
423 and even induce deletions and amplifications (Jablonka and Lamb 2010, see also Asano et  
424 al. 2015). Moreover, the response to the environment would be faster when less mutational  
425 or epi-mutational steps are required in reference to an environmental challenge (e.g., Blount  
426 et al. 2012). This last proposition can explain why in “clonal” bacterial evolutionary  
427 experiments not all colonies respond at the same time to the same environmental challenge,  
428 some respond differently but with similar results and some do not respond at all during the  
429 length of the experiment (e.g., Woods et al. 2006, Stanek et al. 2009, Braun and David  
430 2011, Blount et al. 2012, Cooper 2012). The outcome will depend on exactly the structure  
431 of the genotype network and where on the genotype network evolution started during  
432 experiments.

433

434           Finally, niche construction is another non-Darwinian force imposing novel  
435 challenges on organisms via changes generated on the environment by the same organisms  
436 (Odling-Smee et al., 2003). In other words, changes imposed on the environment by species  
437 modify the adaptive landscape and the n-dimensional genotype network across generations.  
438 Such changes might produce environmental feedbacks on both the same organisms  
439 producing the change and indirectly on those other organisms under the influence of the

440 novel environment. A novel environment will alter the probabilistic nature of the QW,  
441 changing the likelihood of evolutionary pathways (i.e., creating new evolutionary  
442 constraints), which according to our results would be better explored by the diverse  
443 behavior of the QW than CRW.

444

445         The framework presented here provides a probabilistic process (via a quantum wave  
446 function) that might act as the mechanism for the evolutionary exploration of n-dimensional  
447 genotype networks within the constraints established by the available options (i.e.,  
448 phenotypes). In this sense, our study complements the initial work of Ogryzko (1997) and  
449 McFadden and Al-Khalili (1999) by providing an evolutionary context (highly diverse and  
450 robust n-dimensional genotype networks), where a quantum wave function is the  
451 mechanism of evolutionary exploration. The process still needs to be investigated in much  
452 larger n-dimensional genotype networks and also under open system scenarios, where the  
453 environment might influence system's behavior. Such analysis will determine if certain cell  
454 states (quantum superposition) have stronger interactions with current environmental  
455 conditions compared to other states, which subsequently promotes quantum decoherence  
456 toward those more likely options resulting in adaptive mutations (e.g., Asano et al. 2015;  
457 Godbeer et al. 2015). Those likely options will be given by the current genomic context of  
458 the population (i.e., the n-dimensional genotype network), which are not necessarily better  
459 or best for the current conditions, but are most likely in accordance to current context (i.e.,  
460 evolutionary constraints; see Rozen et al. 2008 for a probable example of this effect).

461

462         A way to prove our theory experimentally can be by using clonal bacterial colonies  
463 that start from different positions in the genotype network, in such a way that decoherence

464 times can be measured under the influence of a novel environment (e.g., lactose); such  
465 times should be repeatable across experiments (see Fig. 5). Modern –omics (e.g., genomics,  
466 transcriptomics) and biotechnology techniques can be used to construct specific bacterial  
467 lines for such experiments. In addition, it would be possible to analyze the epi-genome of  
468 plants, which are the organisms where this type of non-Darwinian evolutionary process is  
469 more common.

470

#### 471 Acknowledgements

472 We are grateful to A. Raúl Hernández Montoya for providing computational resources. DS-  
473 A has been continuously supported by the Consejo Nacional de Ciencia y Tecnología de  
474 México (CONACyT project number Ciencia Básica 2011-01-168524 and project number  
475 Problemas Nacionales 2015-01-1628) and the Instituto de Ecología, A.C. S.L.-H.  
476 acknowledges financial support from CONACYT project CB2015-01/255702. SEV-A  
477 acknowledges the financial support of Tecnológico de Monterrey, Escuela de Ingeniería y  
478 Ciencias and of CONACyT (SNI number 41594, as well as Fronteras de la Ciencia project  
479 No. 1007).

480

#### 481 **Figure Legends**

482 **Fig 1.** At the top, (a) shows a correct A-T base pairing, whereas (b) shows an A-T base pair  
483 with their hydrogen protons switched. At the bottom, on the left a correct G-C base pair and  
484 on the right two tautomeric base pairs (modified from McFadden and Al-Kahlili 2014).

485

486 **Fig 2.** Decoherence process of a quantum wave function with three possible states under  
487 the influence of an environmental factor (measurement). **a)** Three possible bacterial cell

488 states (we only use three for simplicity, but it can include all n-dimensional neighbors in a  
489 genotype network, see Fig. 4), represented by state vectors. **b)** Superposition of the three  
490 state vectors, which results in a linear combination of eigen functions each with a  
491 probability  $C_i$ . **c)** The quantum wave function collapses toward the fit cell variant (i). When  
492 measuring time to decoherence (ii) all states of the quantum superposition under no  
493 selective conditions (i.e., no lactose) are indistinguishable by the bacterial cell, eventually  
494 collapsing to any of the possible states at  $T_{D1}$ . However, when the environmental factor is  
495 present (i.e., lactose present) the time to decoherence will be shorter ( $T_{D2}$ ) and biased  
496 toward fit variants (i.e., adaptive mutation) able to grow and reproduce. Those bacterial  
497 cells that do not reduce toward the adaptive state, will remain in a quantum superposition.  
498 Thus, the quantum superposition will collapse to the adaptive state with higher probability  
499 under the environmental adaptive conditions (i.e., lactose present) compared to the time it  
500 takes to appear under non-selective environments ( $T_{D2} < T_{D1}$ ).

501

502 **Fig 3.** a) A list of metabolic reactions, a 1 next to a reaction indicates that an organism has  
503 such a metabolic path otherwise there is a 0. b) A list of resources that can be used (1) or  
504 not (0) by a metabolic genotype in order to synthesize all required biomolecules (see the  
505 text for details; modified from Wagner 2011).

506

507 **Fig 4.** Representation of metabolic genotypes and phenotypes in different dimensions  
508 (modified from Wagner 2011). Networks in one, two, and three dimensions, where vertices  
509 are labeled with the binary strings that correspond to each dimension (1 = presence of  
510 metabolic pathway, 0 = absence of metabolic pathway; see Fig. 3). Two versions of a 3D  
511 representation of a four-dimensional cube are shown (i.e., the shadow of a Tesseract), each

512 with its own section of a genotype network (i.e., network of white circles in upper panel  
513 and network of black circles in lower panel representing different phenotypes). Each line  
514 (i.e., link or edge) connecting two symbols represents a single mutational step. Genotype  
515 networks (those with same symbols) are vast across hyper-dimensions (genotype space),  
516 maintaining the same phenotype (i.e., robust to mutational changes across the network)  
517 even if genotype similarity is low (e.g., nodes on opposite sides of the genotype network).  
518 On the right side, we unfold the 4D cubes into 2D images for clarity. There, neighborhoods  
519 at different places of the genotype space are very diverse (different symbols inside dashed  
520 circles), which opens opportunities to find novel phenotypes. Some of the same  
521 evolutionary novelties can also be found at different neighborhoods, allowing for  
522 convergence. Each genotype network is connected to an n-number of other genotype  
523 networks via extra-dimensional bypasses (black double lines connecting genotype networks  
524 belonging to different phenotypic networks).

525

526 **Fig 5.** A bacterial genotype network under two environments without lactose (top) and with  
527 lactose (bottom). The superpositions of three possible cell states and times to decoherence  
528 are depicted in the middle, to the right of each genotype network (see Fig 2 for details). On  
529 the right hand side, there are three alternative neighborhoods of the original genotype  
530 network shown on the left. Different decoherence times ( $T_D$ ) to reach the genotype capable  
531 of using lactose are illustrated, based on different paths followed on different  
532 neighborhoods of the genotype network. The time to decoherence from the middle network  
533 on the right hand side is shorter compared to the other two (i.e.,  $T_{D3} < T_{D2} < T_{D1}$ ).

534

535 **Fig 6.** A subset of transcription factor genotype networks representing four phenotype  
536 networks (different colors) extracted from Genonets server (Khalid et al. 2016) and used for  
537 simulation analyses via QW and CRW.

538

539 **Fig 7.** Simulation results for two phenotype networks (Foxa2 and Bbx; see Fig. 6).  
540 Probability of mutating to a novel phenotype as a function of time under the CRW (blue  
541 lines) and the QW (red lines) in log-log scale. Upper lines represent the average probability  
542 of simulations started at nodes that were one mutational step away from the novel  
543 phenotype; middle and lower lines are probability averages of nodes two and three  
544 mutational steps away from the novel phenotype, respectively. Shaded areas limited by  
545 dotted lines around the average lines represent the respective standard deviations of each  
546 simulation. The orange shaded area indicates the temporal estimates to decoherence time,  
547 and the vertical gray line is the time of a bacterial cell generation (i.e., approximately 20  
548 minutes).

549

550 **Fig 8.** Simulation results for four phenotype networks (see Fig. 6). Probability of mutating  
551 to a novel phenotype as a function of time under the CRW (left column) and the QW (right  
552 column) in log-log scale. Top panels show results for nodes one mutational step away from  
553 a novel phenotype, middle panels for nodes two mutational steps away from novel  
554 phenotypes, and bottom panels started from three mutational steps away from novel  
555 phenotypes. The color of the different lines indicates the phenotype network where the  
556 simulation started (see Fig. 6). Shaded areas limited by dotted lines around the average  
557 lines represent the respective standard deviations of each simulation. Orange shaded areas



558 indicate the temporal estimates to decoherence time, and the vertical dotted lines are the  
559 time of a bacterial cell generation (i.e., approximately 20 minutes).

560

## 561 **References**

562

563 Aguilar-Rodríguez J, Payne JL, Wagner A. 2017. A thousand empirical adaptive  
564 landscapes and their navigability. *Nature Ecology & Evolution* 1: 0045.

565

566 Asano M, Khrennikov A, Ohya M, Tanaka Y, Yamato I. 2015. Quantum adaptivity in  
567 biology: from genetics to cognition. Springer, Dordrecht

568

569 Badis G, Berger MF, Philippakis AA, Talukder S, Gehrke AR, Jaeger SA, Chan ET,  
570 Metzker G, Vedenko A, Chen X, Kuznetsov H, Wang CF, Coburn D, Newburger DE,  
571 Morris Q, Hughes TR, Bulyk ML. 2009. Diversity and complexity in DNA recognition by  
572 transcription factors. *Science* 324: 1720-1723.

573

574 Balin SJ, Cascalho M. 2010. The rate of mutation of a single gene. *Nucleic Acids Research*.  
575 38: 1575-1582.

576

577 Bastolla U, Porto M, Roman HE, Vendruscolo M. 2003. Connectivity of neutral networks,  
578 overdispersion, and structural conservation in protein evolution. *Journal of Molecular*  
579 *Evolution* 56: 243-254.

580

581 Blount ZD, Barrick JE, Davidson CJ, Lenski RE. 2012. Genomic analysis of a key  
582 innovation in an experimental *Escherichia coli* population. *Nature* 489: 513-518.

583

584 Braun E, David L. 2011. The role of cellular plasticity in the evolution of regulatory  
585 novelty. *In* Transformations of Lamarckism: from subtle fluids to molecular biology  
586 (Gissis, S.B. and E. Jablonka, Editors). MIT Press. Massachusetts, USA. Pp. 181-191.

587

588 Brovarets' OO, Hovorun DM (2015) Proton tunneling in the A·T Watson-Crick DNA base  
589 pair: myth or reality?, *Journal of Biomolecular Structure and Dynamics*, 33: 2716-2720.

590

591 Brookes JC. 2017. Quantum effects in biology: golden rule in enzymes, olfaction,  
592 photosynthesis and magnetodetection. *Proceedings of the Royal Society A* 473: 20160822.

593

594 Cairns J, Overbaugh J, Millar S. 1988. The origin of mutants. *Nature* 335: 142-145.

595

596 Carey, N. 2012. *The epigenetics revolution*. Columbia University Press, New York.

597

598 Ciliberti S, Martin OC, Wagner A. 2007. Robustness can evolve gradually in complex  
599 regulatory gene networks with varying topology. *PLoS Computational Biology* 3: e15.

600

601 Cooper TF. 2012. Empirical insights into adaptive landscapes from bacterial experimental  
602 evolution. *In* The adaptive landscape in evolutionary biology (Svensson, E.I., and Calsbeek,  
603 R., Editors). Oxford Univ. Press. Oxford, U.K. Pp. 169-179.

604

605 Cui Y, Wong W, Bornberg-Bauer E, Chan H. 2002. Recombinatoric exploration of novel  
606 folded structures: a heteropolymer-based model of protein evolutionary landscapes.  
607 Proceedings of the National Academy of Sciences USA 99: 809-814.  
608  
609 Djordjevic IV. 2016. Quantum biological information theory. Springer, Cham.  
610  
611 Espinosa-Soto C, Martin OC, Wagner A. 2011. Phenotypic robustness can increase  
612 phenotypic variability after nongenetic perturbations in gene regulatory circuits. Journal of  
613 Evolutionary Biology 24: 1284-1297.  
614  
615 Falloon PE, Rodriguez J, Wang JB. 2017. QSWalk: a Mathematica package for quantum  
616 stochastic walks on arbitrary graphs. Computer Physics Communications 217: 162-170.  
617  
618 Farhi E, Gutmann S. (1998). Quantum computation and decision trees. Physical Review A  
619 58: 915–929.  
620  
621 Godbeer AD, Al-Khalili JS, Stevenson PD. 2015. Modelling proton tunneling in the  
622 adenine-thymine base pair. Physical Chemistry Chemical Physics 17: 13034.  
623  
624 Hall BG. 1995. Adaptive mutations in *Escherichia coli* as a model for the multiple  
625 mutational origins of tumors. Proceedings of the National Academy of Sciences USA 92:  
626 5669-5673.  
627  
628 Hall BG. 1997. Spontaneous point mutations that occur more often when advantageous

629 than when neutral. *Genetics* 126: 5-16.

630

631 Hall BG. 1998. Adaptive mutagenesis at *ebgR* is regulated by PhoPQ. *Journal of*  
632 *Bacteriology* 180: 2862-2865.

633

634 Hendrickson H, Slechta ES, Bergthorsson U, Andersson DI, Roth JR. 2002. Amplification-  
635 mutagenesis: evidence that “directed” adaptive mutation and general hypermutability result  
636 from growth with a selected gene amplification. *Proceedings of the National Academy of*  
637 *Sciences USA* 99: 2164-2169.

638

639 Jablonka E, Raz G. 2009. Transgenerational epigenetic inheritance: prevalence,  
640 mechanisms, and implications for the study of heredity and evolution. *Quarterly Review of*  
641 *Biology* 84: 131-176.

642

643 Jablonka E, Lamb MJ. 2010. Transgenerational epigenetic inheritance *In* *Evolution the*  
644 *extended synthesis* (Pigliucci, M. and Müller, G.B., Editors). MIT Press. Cambridge, MA.  
645 USA. Pp. 137-174.

646

647 Jablonka E. 2011. Cellular epigenetic inheritance in the twenty-first century. *In*  
648 *Transformations of Lamarckism: from subtle fluids to molecular biology* (Gissis, S.B. and  
649 E. Jablonka, Editors). MIT Press. Massachusetts, USA. Pp. 215-226.

650

651 Kempe J (2003) Quantum random walks: An introductory overview, *Contemporary Physics*  
652 44: 307-327.

653

654 Khalid F, Aguilar-Rodríguez J, Wagner A, Payne JL 2016. Genonets server – a web server  
655 for the construction, analysis and visualization of genotype networks. *Nucleic Acids*  
656 *Research* 44: W70-W76.

657

658 Klinman JP, Kohen A. 2013 Hydrogen tunneling links protein dynamics to enzyme  
659 catalysis. *Annual Review of Biochemistry* 82: 471-496.

660

661 Li H, Helling R, Tang C, Wingreen N. 1996. Emergence of preferred structures in a simple  
662 model of protein folding. *Science* 273: 666-669.

663

664 Livnat A. 2013. Interaction-based evolution: how natural selection and nonrandom  
665 mutation work together. *Biology Direct* 8: 24.

666

667 Lloyd S. 2008. Quantum mechanics and emergence. *In* *Quantum aspects of life* (Abbott,  
668 D., Davies, P.C.W., and Pati, A.K., Editors). Imperial College Press. London, UK., pp. 19-  
669 30.

670

671 Mandelstam L, Tamm I. 1945. The uncertainty relation between energy and time in  
672 nonrelativistic quantum mechanics. *Journal of Physics (USSR)* 9:249-254.

673

674 Martin-Delgado JA. 2012. On quantum effects in a theory of biological evolution. *Sci. Rep.*  
675 2:302. DOI: 10.1038/srep00302

676

677 McFadden J, Al-Khalili J. 1999. A quantum mechanical model of adaptive mutation.  
678 *BioSystems* 50: 203-211.  
679  
680 McFadden J, Al-Khalili J. 2014. *Life on the edge: the coming of age of quantum biology*.  
681 Crown Publishers. New York, NY.  
682  
683 McFadden J, Al-Khalili J. 2018 The origins of quantum biology. *Proceedings of the Royal*  
684 *Society of London A* 474: 20180674.  
685  
686 Mohseni M, Omar Y, Engel G, Plenio M (Eds.). 2014. *Quantum effects in biology*.  
687 Cambridge University Press. Cambridge, UK.  
688  
689 Mülken O, Blumen A. 2011. Continuous-time quantum walks: models for coherent  
690 transport on complex networks. *Physics Reports* 502:37-87.  
691  
692 Nijhout HF. 2003. Development and evolution of adaptive polyphenisms. *Evolutionary*  
693 *Development*. 5: 9-18.  
694  
695 Odling-Smee FJ, Laland KN, Feldman MW. 2003. *Niche Construction: the neglected*  
696 *process in evolution*. Princeton Univ. Press. Princeton, NJ, USA.  
697  
698 Ogryzko VV. 1997. A quantum-theoretical approach to the phenomenon of directed  
699 mutations in bacteria (hypothesis). *BioSystems* 43: 83-95.  
700

701 Palmer AR. 2012. Developmental plasticity and the origin of novel forms:  
702 unveiling cryptic genetic variation via “use and disuse”. *Journal of Experimental Zoology*  
703 *B: Molecular and Developmental Evolution* 318: 466-479.  
704  
705 Panitchayangkoon G, Hayes D, Fransted KA, Caram JR, Harel E, Wen J, Blankenship RE,  
706 Engel GS. 2010. Long-lived quantum coherence in photosynthetic complexes at  
707 physiological temperature. *Proceedings of the National Academy of Sciences USA* 107:  
708 12766-12770.  
709  
710 Payne JL, Wagner A. 2014. The robustness and evolvability of transcription factor binding  
711 sites. *Science* 343: 875-877.  
712  
713 Rassoulzadegan M. 2011. An evolutionary role for RNA-mediated epigenetic variation? *In*  
714 *Transformations of Lamarckism: from subtle fluids to molecular biology* (Gissis, S.B. and  
715 E. Jablonka, Editors). MIT Press. Massachusetts, USA. Pp. 227-235.  
716  
717 Rodrigues JFM, Wagner A. 2009. Evolutionary plasticity and innovations in complex  
718 metabolic reaction networks. *Plos Computational Biology* 5:e1000613.  
719  
720 Rodrigues JFM, Wagner A. 2011. Genotype networks, innovation, and robustness in sulfur  
721 metabolism. *BMC Systems Biology* 5:39  
722  
723 Rosenberg SM, Longrich S, Gee P, Harris RS. 1994. Adaptive mutation by deletions in  
724 small mononucleotide repeats. *Science* 265: 405-407.

725

726 Rozen DE, Habets MGJL, Handel A, de Visser JAGM (2008) Heterogeneous Adaptive  
727 Trajectories of Small Populations on Complex Fitness Landscapes. PLoS ONE 3(3): e1715.

728

729 Samal A, Rodrigues JFM, Jost J, Martin OC, Wagner A. 2010. Genotype networks in  
730 metabolic reaction spaces. BMC Systems Biology 4:30.

731

732 Samal A, Wagner A, Martin OC. 2011. Environmental versatility promotes modularity in  
733 genome-scale metabolic networks. BMC Systems Biology 5:135.

734

735 Schrödinger E. 1944. What is Life? Cambridge University Press, London.

736

737 Schuster P, Fontana W, Stadler P, Hofacker I. 1994. From sequences to shapes and back – a  
738 case-study in RNA secondary structures. Proceedings of the Royal Society of London B  
739 255: 279-284.

740

741 Stanek MT, Cooper TF, Lenski RE. 2009. Identification and dynamics of a beneficial  
742 mutation in a long-term evolution experiment with *Escherichia coli*. BMC Evolutionary  
743 Biology 9: 302.

744

745 Stumpf JD, Poteete AR, Foster PL. 2007. Amplification of *lac* cannot account for adaptive  
746 mutation to Lac<sup>+</sup> in *Escherichia coli*. Journal of Bacteriology 189:2291-2299.

747



748 Sumedha, Martin, OC, Wagner A. 2007. New structural variation in evolutionary searchers  
749 of RNA neutral networks. *Biosystems* 90: 475-485.  
750

751 Venegas-Andraca SE. 2012. Quantum walks: a comprehensive review. *Quantum*  
752 *Information Processing* 11:1015-1106.  
753

754 Wagner A. 2008. Robustness and evolvability: a paradox resolved. *Proceedings of the*  
755 *Royal Society of London B* 275: 91-100.  
756

757 Wagner A. 2009. Evolutionary constraints permeate large metabolic networks. *BMC*  
758 *Evolutionary Biology* 9: 231.  
759

760 Wagner A. 2011. *The origins of evolutionary innovations: a theory of transformative*  
761 *change in living systems*. Oxford Univ. Press. New York. USA.  
762

763 Wagner A. 2012. The role of randomness in Darwinian evolution. *Philosophy of Science*  
764 79:95-119.  
765

766 Wagner A. 2014. *Arrival of the fittest: solving evolution's greatest puzzle*. Current. New  
767 York, USA.  
768

769 Watson JD, Crick FHC. 1953a. Molecular structure of nucleic acids: a structure for  
770 deoxyribose nucleic acid. *Nature* 171: 737-738.  
771

772 Watson JD, Crick FHC. 1953b. Genetical implications of the structure of deoxyribonucleic  
773 acid. *Nature* 171: 964-967.

774

775 Wolfram Research, Inc. 2020. *Mathematica*, v12.1, Champaign, USA.

776

777 Woods R, Schneider D, Winkworth CL, Riley MA, Lenski RE. 2006. Tests of parallel  
778 molecular evolution in a long-term experiment with *Escherichia coli*. *Proceedings of the*  
779 *National Academy of Sciences USA* 103: 9107-9112.

780

#### 781 **Data, Code and Materials**

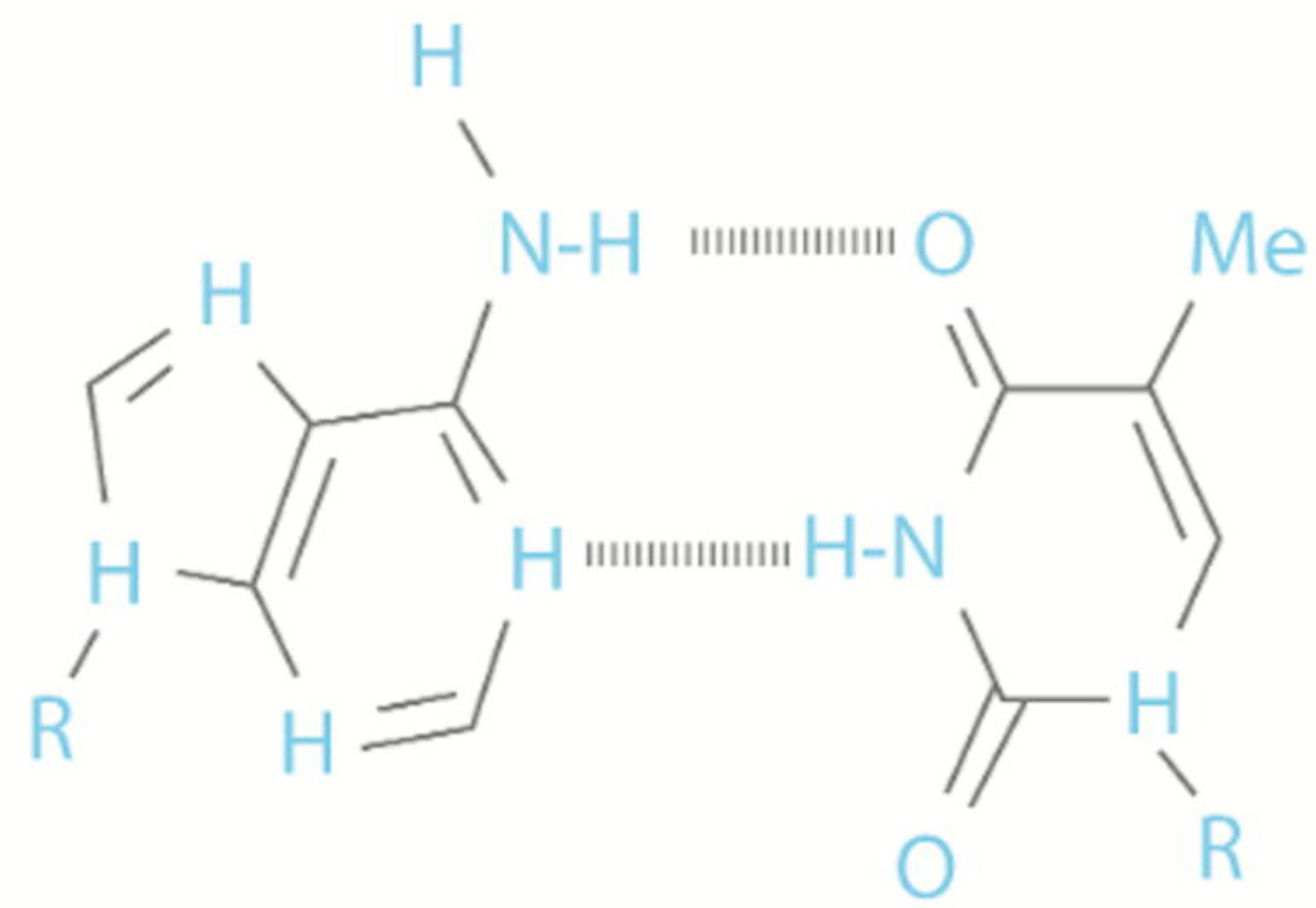
782 The Mathematica code and data used for simulations supporting results of this article are  
783 available upon request to [htapia@uv.mx](mailto:htapia@uv.mx) and will be publicly stored in figshare.com once  
784 the paper is published. See also supplementary material.

#### 785 **Competing interests**

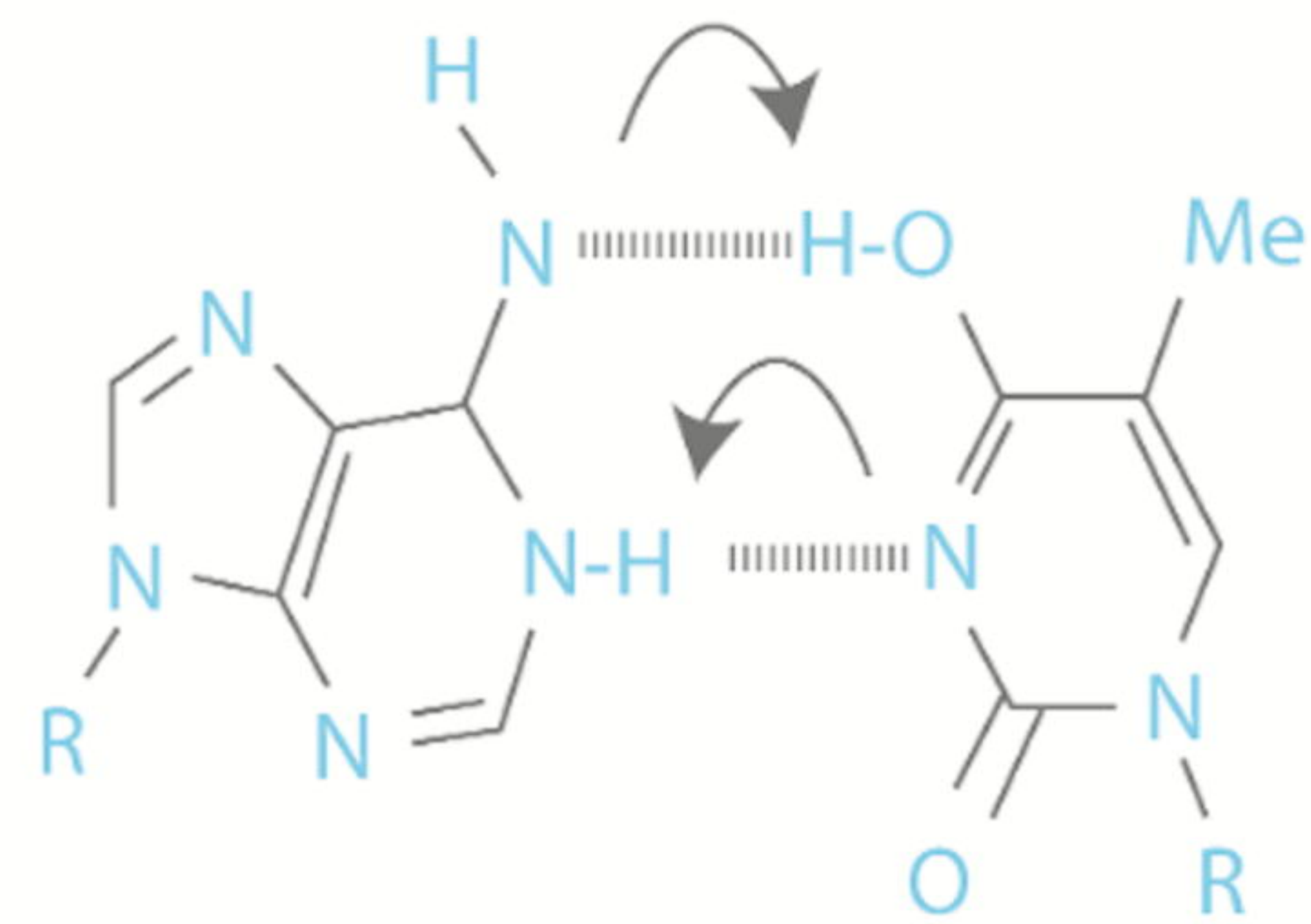
786 Authors declare to have no competing interests.

#### 787 **Authors' contributions**

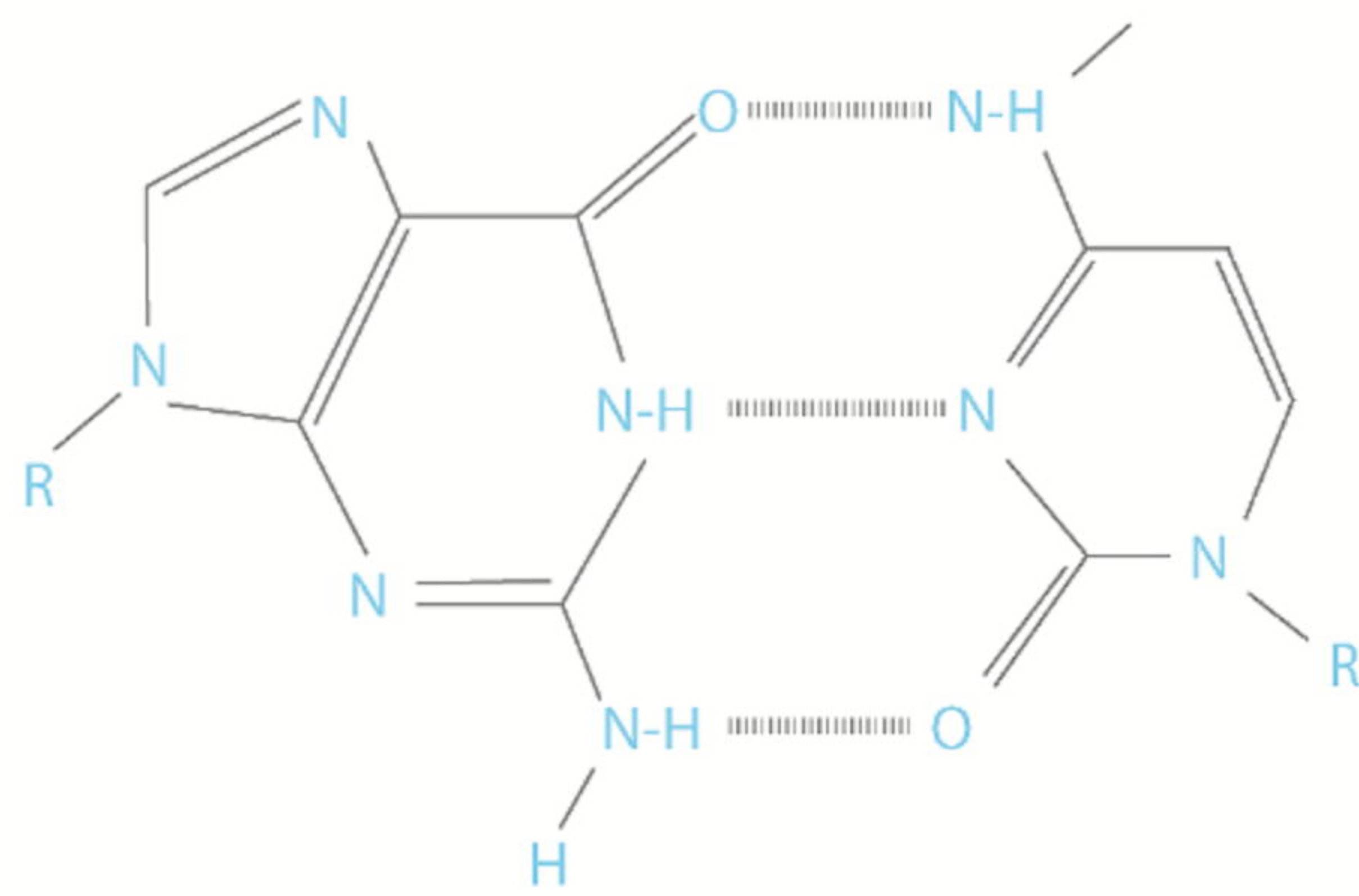
788 DS-A developed the idea and drafted the manuscript; DS-A, HT-Mc, and SL-H refined the  
789 concept and designed the simulations; HT-Mc and SL-H performed the simulations and  
790 helped draft the manuscript. SEV-A refined the idea, formalized the quantum random walks  
791 mathematics, and helped draft the manuscript. All authors gave final approval for  
792 publication and agreed to be held accountable for the work performed therein.



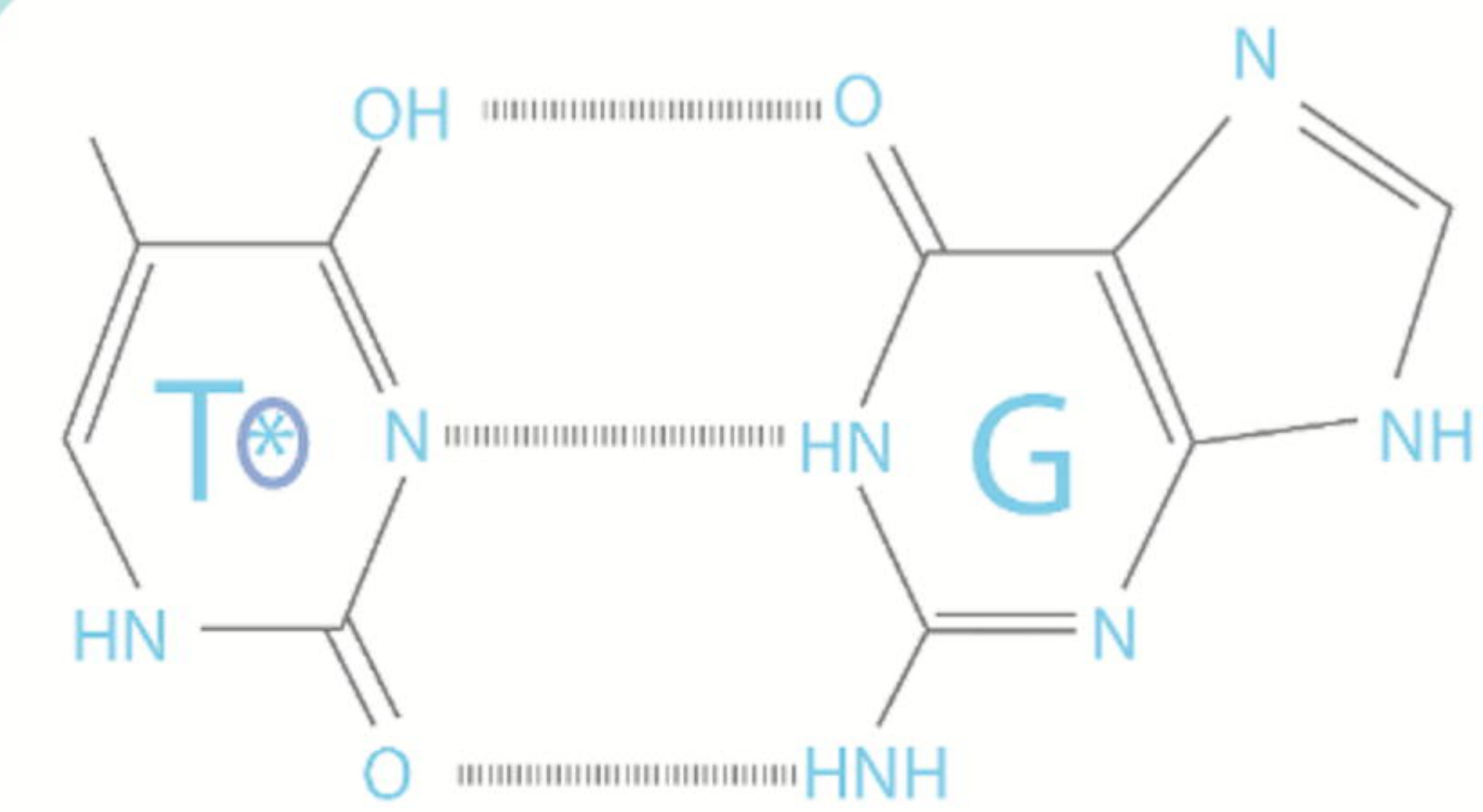
A-T base pair (a)



A-T base pair (b)

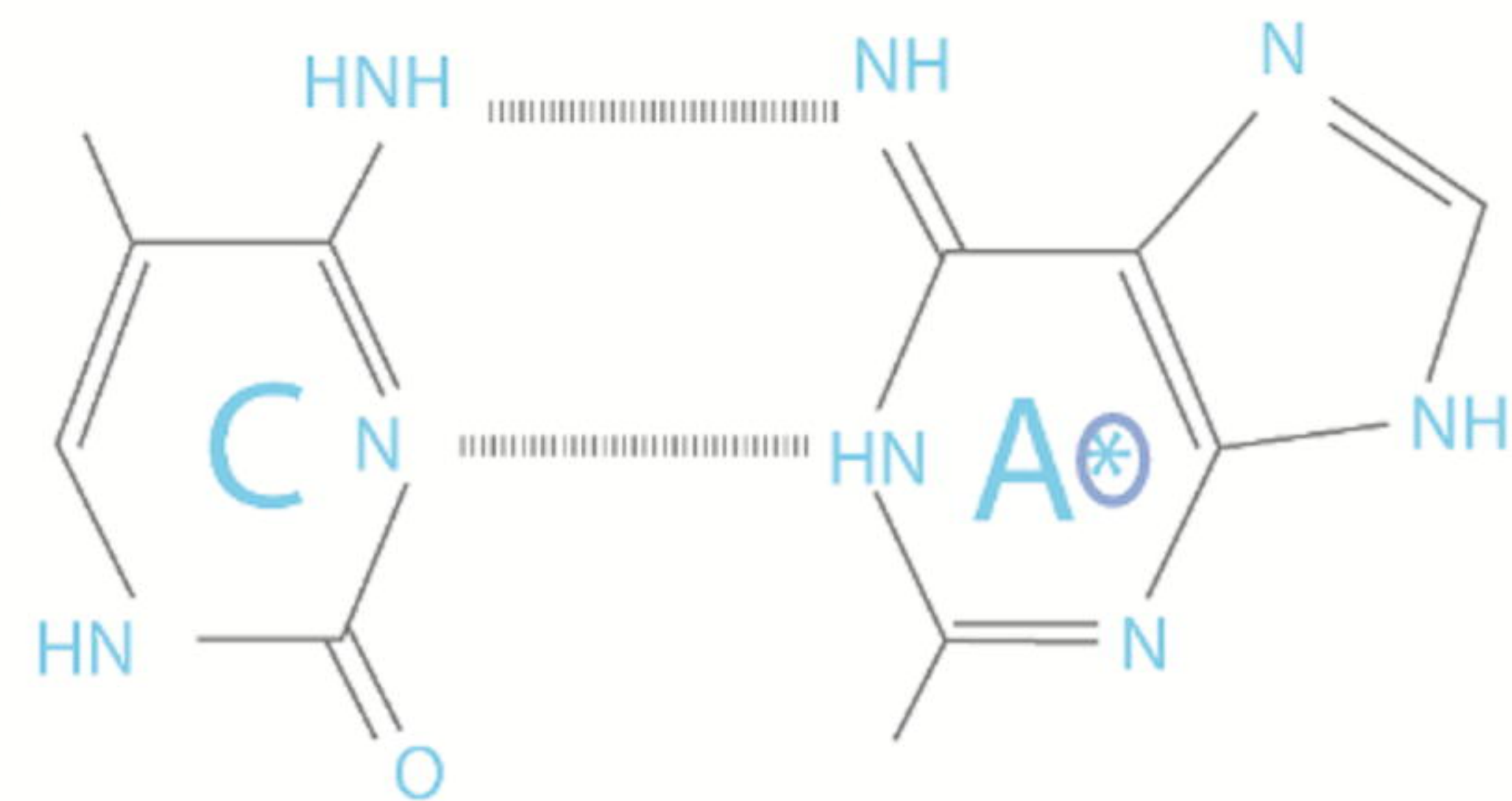


G-C base pair



Thymine

Guanine



Cytosine

Adenine

Tautomeric base pairs

a) Eigen Functions

$|\psi_1\rangle =$  cell death,  $|\psi_2\rangle =$  stationary cell state;  $|\psi_3\rangle =$  reproduction on novel environment

b) Superpositions of Eigen Functions

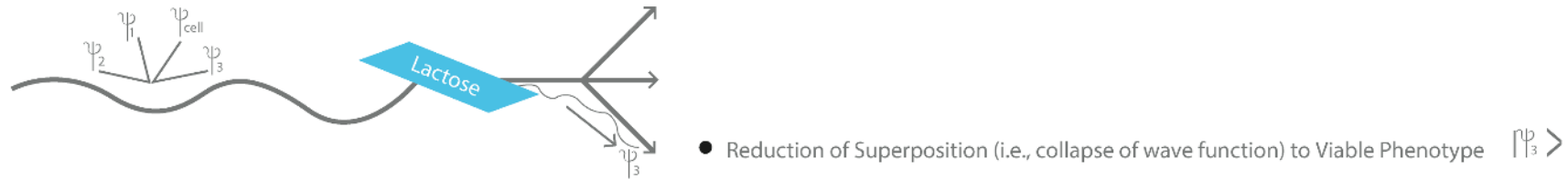
$|\psi\rangle = C_1|\psi_1\rangle + C_2|\psi_2\rangle + C_3|\psi_3\rangle$   $C_i =$  probability coefficients

Linear combination of possible states in a n-dimensional genotype space

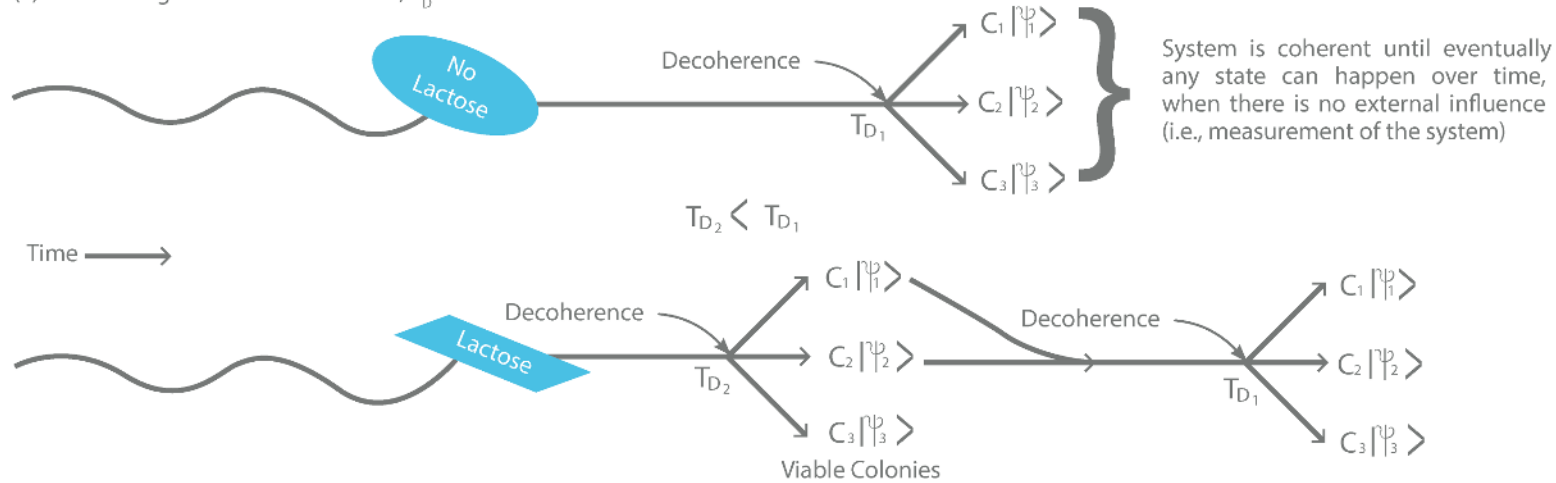
$$|\psi\rangle = \sum a_i |\psi_i\rangle$$

c) Under a Selective Environment

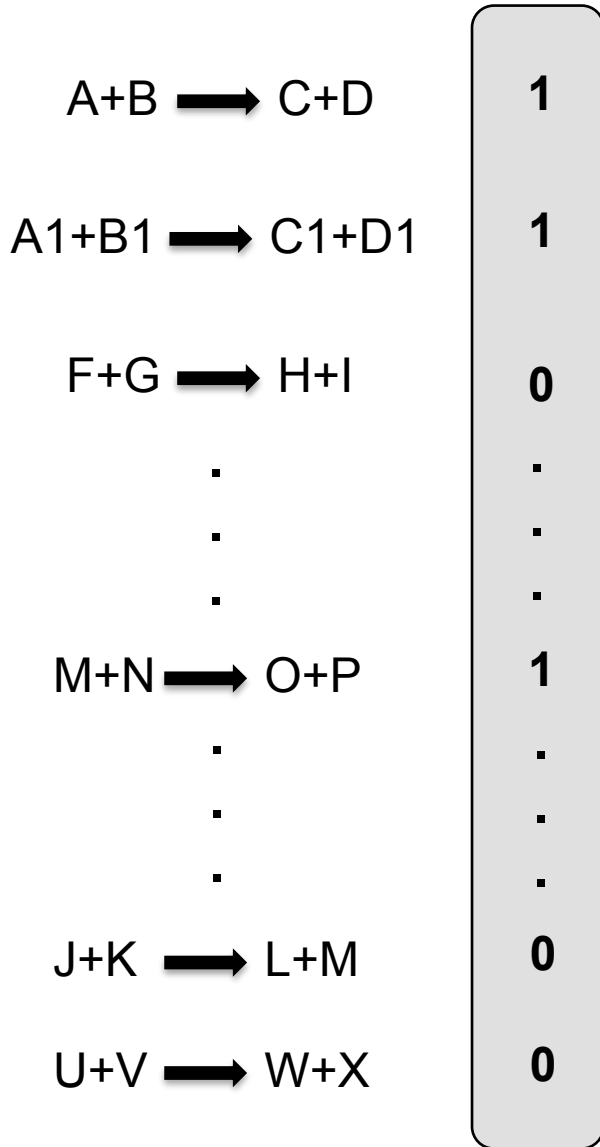
(i) Lactose  $|\psi_{\text{cell}}\rangle = C_1|\psi_1\rangle + C_2|\psi_2\rangle + C_3|\psi_3\rangle$



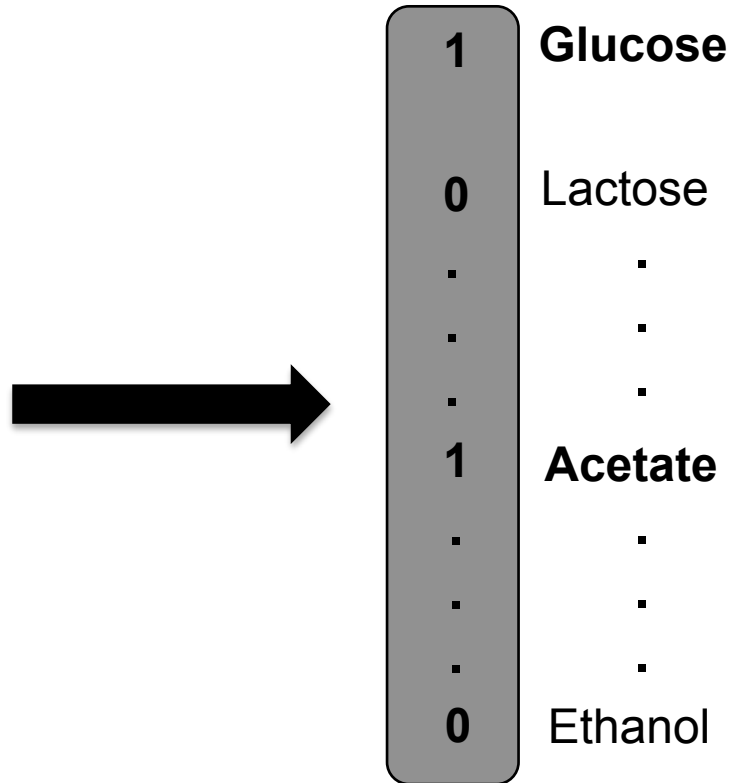
(ii) Considering Time to Decoherence;  $T_D =$  time to decoherence



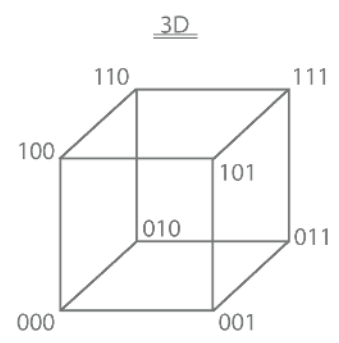
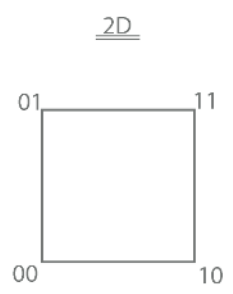
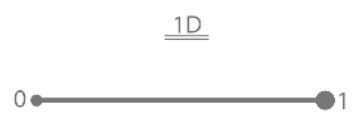
a) Metabolic Genotype (e.g., network of enzymatic reactions or of transcription factors)



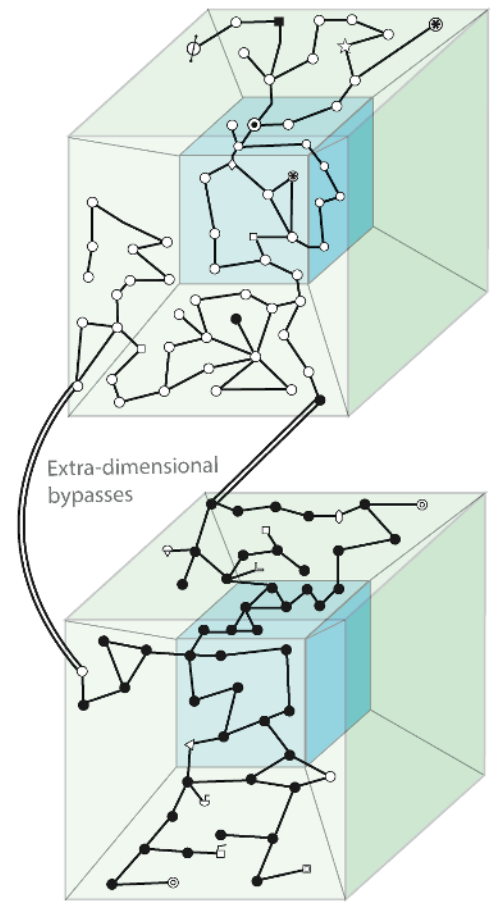
b) Metabolic Phenotype (e.g., viability of metabolic genotype on different resources)



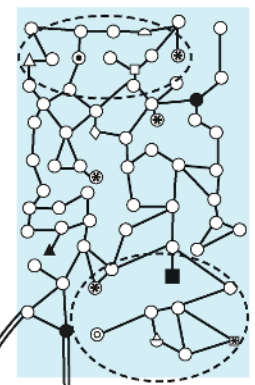




Genotype Networks in a 3D Representation of a 4D Cube



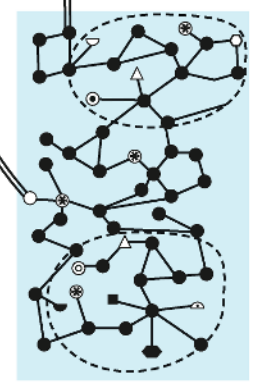
Unfolding the n-dimensions in 2D for clarity



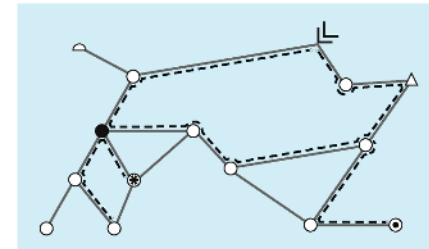
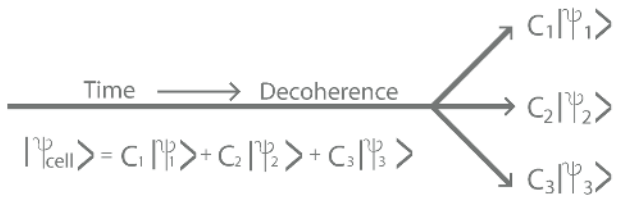
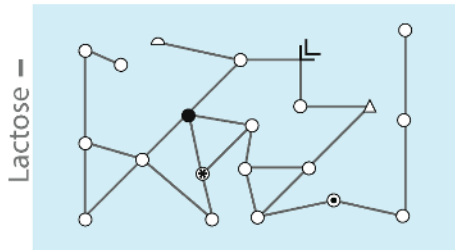
Genotype Space

Genotype networks traversing deep throughout the n-dimensional genotype space.

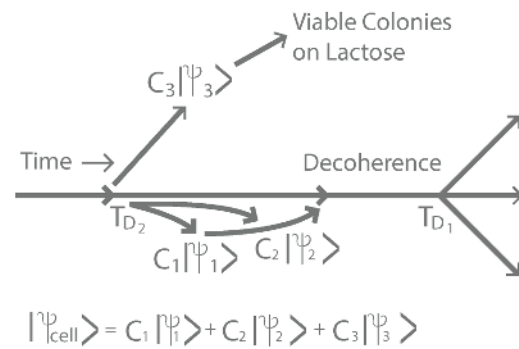
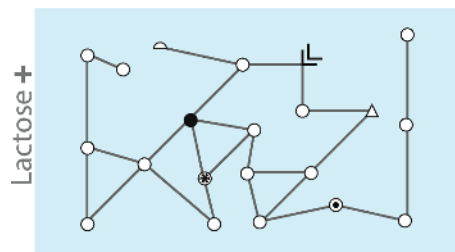
Unfolding the n-dimensions in 2D for clarity



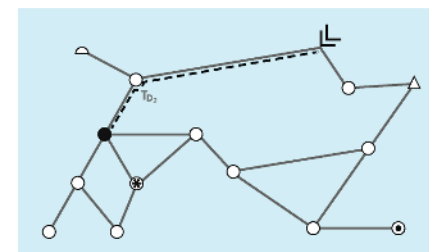
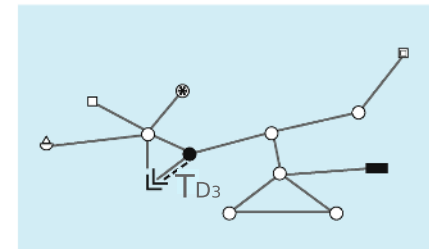
Dashed polygons show the diverse neighborhoods that can be found in different parts of genotype space, and also that same solutions can be found across the hyperdimensional space.



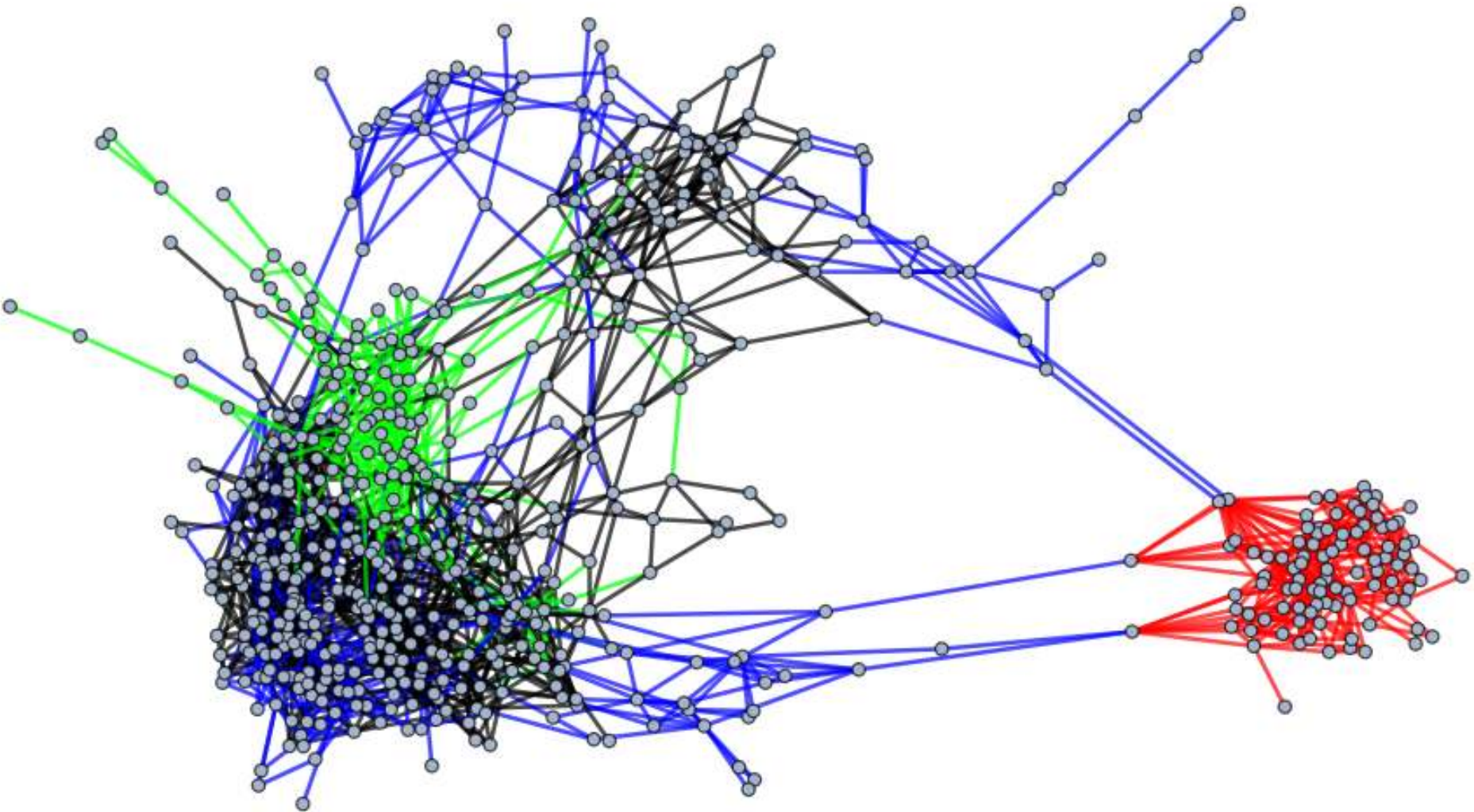
- ⊥ = Genotype capable of using lactose
- = Initial genotype of the bacterial population
- = Paths to novel adaptive genotype



$$T_{D_3} < T_{D_2} < T_{D_1}$$

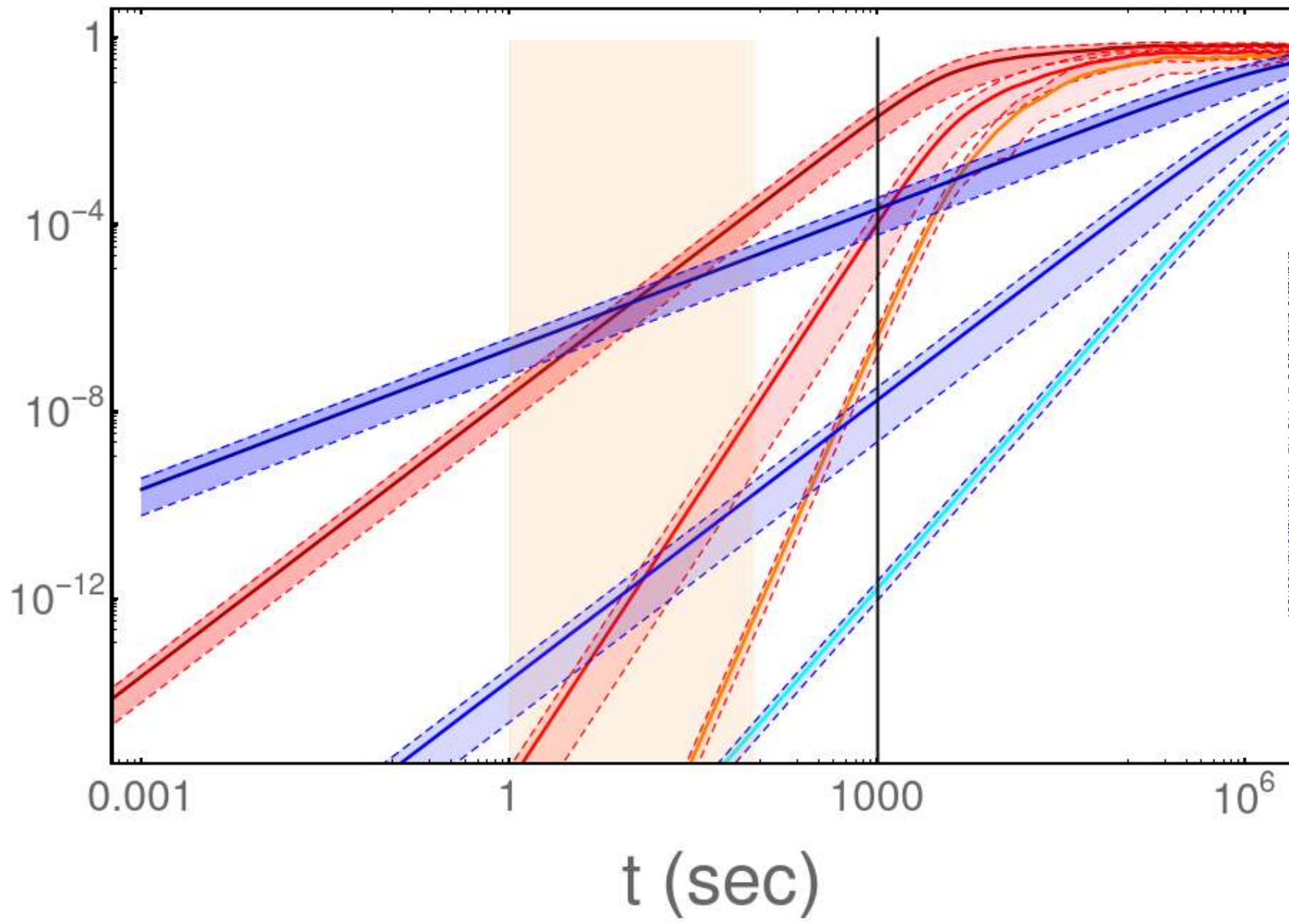


Alternative neighborhoods of same genotype network





Prob



bioRxiv preprint doi: <https://doi.org/10.1101/2020.07.10.197667>; this version posted July 16, 2020. The copyright holder for this preprint (which was not certified by peer review) is the author/funder, who has granted bioRxiv a license to display the preprint in perpetuity. It is made available under aCC-BY-NC-ND 4.0 International license.

